The Tilecal Energy Reconstruction for Collision Data Using the Matched Filter

Bernardo S. Peralva, *Student Member, IEEE,* on behalf of the ATLAS Collaboration

***Abstract*—The Tile Barrel Calorimeter (TileCal) is the central section of the hadronic calorimeter of ATLAS at LHC. It comprises more than 10,000 readout channels. The energy deposited in each channel is read out and the analog pulse is conditioned by a shaper circuit. The signal energy is estimated by reconstructing the amplitude of the digitized pulse sampled every 25 ns. This work presents the performance of an alternative algorithm for TileCal energy reconstruction, namely the TileCal Matched Filter (MF). The performance of the MF method is compared to the currently implemented algorithm (OF2) using collision data acquired in 2010 during LHC operation period. The results showed that the MF presents smaller error estimation (variance) than the OF2 method. In addition to that, the methods showed to be highly correlated with each other for high SNR signals. Preliminary results using special ATLAS collision data taken later in 2012, for which LHC operated at 25 ns bunch spacing and ATLAS observed an increase of the pile-up effect, are also provided.**

ATL-TILECAL-PROC-2013-023
18 November 2013

I. Introduction

ATLAS (A Toroidal LHC ApparatuS) [1] is one of the four main experiments at the LHC and one of two general purpose detectors designed for precision Standard Model measurements and to search for physics beyond the Standard Model. It is composed of six different subsystems: The Inner Detector, the Solenoidal Magnet that surrounds the inner detector, the Electromagnetic and Hadronic calorimeters, the Toroid Magnets and the Muon Spectrometer, as illustrated in Figure 1.

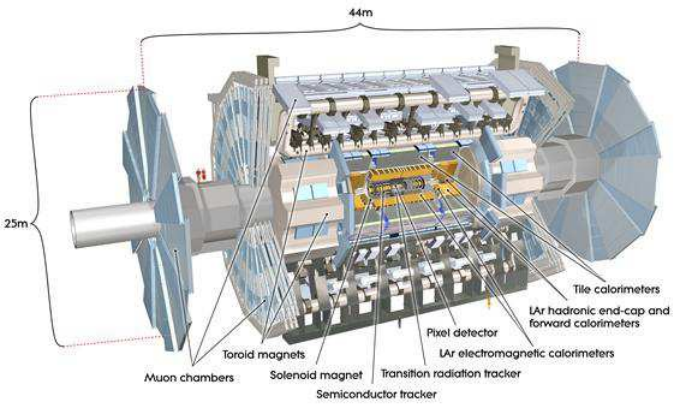

Fig. 1. The ATLAS detector and its subsystems.

Manuscript received November 14, 2013. This work was supported by CNPq, CAPES, RENAFAE, FAPERJ and FAPEMIG (Brazil).

Bernardo S. Peralva is with the Federal University of Juiz de Fora, Juiz de Fora, MG, Brazil (telephone: +55 32 2102 3462, e-mail: bernardo@cern.ch).

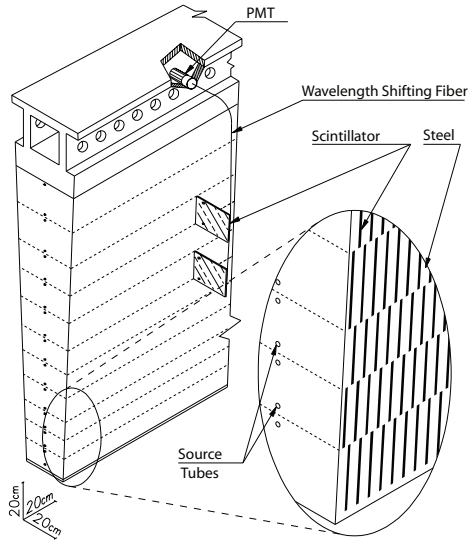

Fig. 2. Schematic diagram showing the mechanical assembly and the optical readout of the Tile Calorimeter, corresponding to a ϕ wedge.

The ATLAS Tile Calorimeter (TileCal) [2] is the main hadronic calorimeter of the ATLAS detector. The aim of TileCal is to perform precise measurements of hadrons, jets, taus and to contribute to the reconstruction of the missing transverse energy as well as to provide input signals to ATLAS online trigger [3]. It consists of three cylinders, one long barrel (LB) splitted into two readout partitions, LBA and LBC (LBs), and two extended barrels (EBs), EBA and EBC, covering the most central region $|\eta| < 1.7$ of ATLAS.

TileCal is a sampling device that uses iron plates as absorber and plastic scintillating tiles as the active material. The particles produced in the interaction point travel through the calorimeter and the light produced in the scintillating tiles is proportional to the energy deposited by the particles. The light is transmitted by wavelength shifting fibers and read out by photomultiplier tubes (PMTs), which generate analog pulses. Figure 2 shows the structure and the signal collection system of one of the 256 ϕ wedges of TileCal.

Each of TileCal central and extended barrel modules are divided, respectively, into 23 and 16 cells with double readout, resulting in almost 10,000 channels. Furthermore, each barrel is divided into 64 modules in azimuth, ϕ, giving a granularity of $\Delta\phi$ of 0.1. Each module is further radially segmented in three layers of readout cells with a granularity of $\Delta\eta$ of 0.1 for the first two layers and $\Delta\eta$ of 0.2 for the third one. The cells belonging to each $\Delta\eta$ slice are summed up to form the so called Trigger Towers and this compact information is sent

to the Level One Calorimeter trigger. The cell segmentation is shown in Figure 3 for a half of a LB module and an EB module.

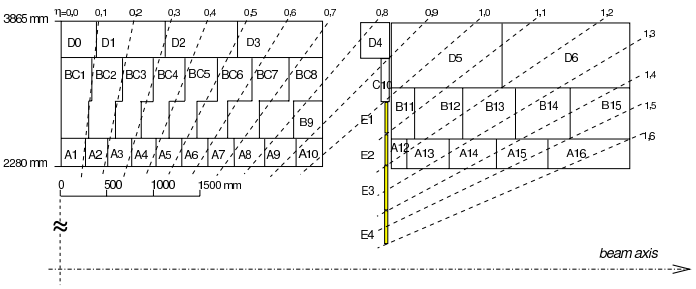

Fig. 3. Schematic view of TileCal cell segmentation for a LB and an EB modules.

The fast pulse generated in the PMT is conditioned by a shaper circuit [4], which provides a 50 ns Full Width at Half Maximum (FWHM) pulse whose the amplitude is proportional to the deposited energy. Therefore, the TileCal pulse shape can be considered almost invariant from channel to channel [5] and the energy deposited by the particle at a given cell can be retrieved by the corrected estimation of the TileCal pulse amplitude.

In order to cover the entire energy range (220 MeV to 1.3 TeV), the shaped pulse is amplified by two operational amplifiers with a gain ratio of 64. The analog signals are converted into digital samples with a 40 MHz sampling clock at the digitizer board. A window of seven samples (150 ns) covers the entire pulse and is readout at every event. The TileCal analog signal as well as its parameters can be seen in Figure 4. The seven samples are represented by the dots spaced 25 ns from each other.

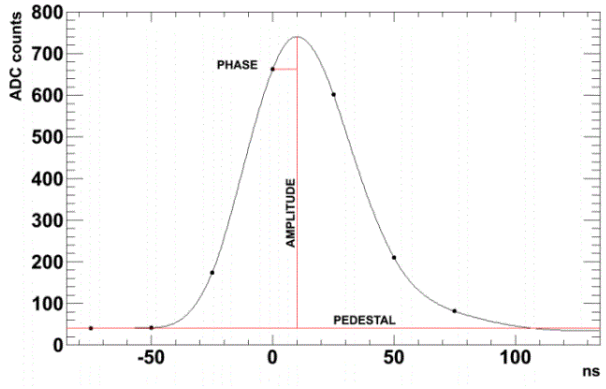

Fig. 4. TileCal reference pulse shape.

The pedestal is defined as the baseline of the signal and the amplitude A is the height of the signal measured from the pedestal. The signal phase is defined as the distance between the pulse peak and the expected time, which is tuned to match the fourth sample. The seven samples from each TileCal channel are transmitted through optical fibers up to the readout drivers (RODs).

II. TileCal Energy Reconstruction

The baseline algorithm for energy reconstruction in ATLAS calorimeter systems is the so called Optimal Filter (OF) [6]. It is a variance minimization technique that makes use of the knowledge of the pulse shape taken from the shaping circuit to estimate the pulse amplitude [7]. Since the background of ATLAS calorimeters comprises only electronic noise, which is often modeled by a Gaussian distribution, the OF is extensively employed in such experiments [8].

The OF version implemented in TileCal is called OF2 [9] and it is the currently used algorithm to estimate the signal amplitude and to reconstruct the energy at the ROD level during detector operation. It makes use of a weighted linear combination of the signal samples to obtain the amplitude of the pulse, according to Equation (1).

$$\hat{A}_{OF} = \sum_{k=0}^{N-1} a_k s_k \tag{1}$$

The weights a_k are obtained from the channel pulse shape and the noise covariance matrix. The procedure aims at minimizing the variance of the amplitude distribution. Thus, they are optimal for deterministic signals corrupted by Gaussian noise. The correct weights are computed by minimizing the effect of the noise in all amplitude, phase and pedestal reconstructions [9].

In order to compute the OF2 weights a_k, the TileCal signal is modeled as a first order approximation:

$$s_k = Ag_k - A\tau g'_k + n_k + ped \qquad k = 0, 1, 2, ..., N-1 \tag{2}$$

where s_k represents the received digital sample k and N is the total number of samples available, which is currently 7 for TileCal. The amplitude A is the parameter to be estimated while n_k is the background noise. The parameters g_k and g'_k are the TileCal reference pulse shape and its derivative (linear approximation for the pulse phase), respectively, while the parameter τ is the signal phase. The variable ped corresponds to the signal pedestal and is a constant value added to the analog signal just before its analog-to-digital conversion.

For a linear and unbiased estimator, it is required that the expectation value of $\hat{A}$ to be A, therefore Equation (3) can be derived.

$$E[\hat{A}_{OF}] = \sum_{k=0}^{N-1} (Aa_k g_k - A\tau a_k g'_k + a_k ped) \tag{3}$$

Since the mean noise value will be zero ($E[n_k] = 0$), the following constraints are deduced in order to be pedestal and phase independent:

$$\sum_{k=0}^{N-1} a_k g_k = 1 \tag{4}$$

$$\sum_{k=0}^{N-1} a_k g'_k = 0 \tag{5}$$

$$\sum_{k=0}^{N-1} a_k = 0 \tag{6}$$

The estimator variance is given by,

$$var(\hat{A}_{OF}) = \sum_{k=0}^{N-1} \sum_{j=0}^{N-1} a_k a_j C_{kj} = \mathbf{a}^T \mathbf{C} \mathbf{a} \quad (7)$$

where $\mathbf{C}$ corresponds to the noise covariance matrix and $\mathbf{a}$ is the vector of weights.

Hence, to find the OF2 weights, Equation (7) is minimized subject to the constraints expressed by Equations (4), (5) and (6) using Lagrange multipliers [6].

III. The TileCal Matched Filter Method

The OF2 method is a constrained minimum variance estimator. Besides that, it builds its detection threshold based on the amplitude estimates in order to select signals of interest. Unlike OF2 method, MF starts from the detection point of view to come up with its coefficients.

A. Signal detection

Due to the high segmentation of the TileCal (around 10,000 channels), not all channels in every event will have relevant information to process. Consequently, a signal detection algorithm against noise can be developed. The detection problem can be described as an hypothesis testing on the received signal:

$$\begin{array}{ll} H_0 : r_k = n_k & k = 0, 1, 2, ..., N-1 \\ H_1 : r_k = g_k + n_k & k = 0, 1, 2, ..., N-1 \end{array} \quad (8)$$

where H_0 represents the null-signal hypothesis while H_1 corresponds to the full-signal hypothesis. By considering $\mathbf{r}$ a given outcome at the receiver end, based on the Neyman-Pearson Lemma, the relationship that maximizes the detection efficiency is given by the likelihood ratio test [10], [11] shown by Equation (9).

$$\Lambda(\mathbf{r}) = \frac{L(H_1|\mathbf{r})}{L(H_0|\mathbf{r})} \underset{H_0}{\overset{H_1}{\gtrless}} \gamma \quad (9)$$

The terms $L(H_1|\mathbf{r})$ and $L(H_0|\mathbf{r})$ are the likelihood functions for the null-signal hypothesis H_0 and full-signal hypothesis H_1 given the data $\mathbf{r}$ was received. The parameter γ is a detection threshold. The idea is to decide in favor of hypothesis H_1 if the likelihood ratio of the received signal is greater than the detection threshold, and otherwise in favor of H_0. In such a way, the likelihood ratio maximizes the detection probability and minimizes the detection error probability.

The likelihood functions are usually unknown for the majority of the real detection problems. Therefore, the detection algorithm should estimate $L(H_1|\mathbf{r})$ and $L(H_0|\mathbf{r})$ from a set of known data. In a multi-variate detection problem, if the variables can be modeled for both H_0 and H_1 hypotheses, the likelihood ratio test can be computed. However, a pre-processing step (typically, a whitening filter) is often needed in order to make noise samples statistically independent from each other.

In the case where the noise is Gaussian and the signal vector $\mathbf{g}$ is deterministic, the estimation of the covariance matrix $\mathbf{C}$ is enough to characterize the signals. Thus, the multivariate Gaussian function is used to model both the null-signal and full-signal likelihood functions. As a result, the likelihood functions $L(H_1|\mathbf{r})$ and $L(H_0|\mathbf{r})$ are defined by Equations (10) and (11), respectively.

$$L(H_1|\mathbf{r}) = \frac{1}{\sqrt{(2\pi)^N |\mathbf{C}|}} \exp\left(-\frac{1}{2}(\mathbf{r}-\mathbf{g})^T \mathbf{C}^{-1} (\mathbf{r}-\mathbf{g})\right) \quad (10)$$

$$L(H_0|\mathbf{r}) = \frac{1}{\sqrt{(2\pi)^N |\mathbf{C}|}} \exp\left(-\frac{1}{2}\mathbf{r}^T \mathbf{C}^{-1} \mathbf{r}\right) \quad (11)$$

Thus, the likelihood ratio test becomes:

$$\Lambda(\mathbf{r}) = \frac{\exp\left(-\frac{(\mathbf{r}-\mathbf{g})^T \mathbf{C}^{-1} (\mathbf{r}-\mathbf{g})}{2}\right)}{\exp\left(-\frac{\mathbf{r}^T \mathbf{C}^{-1} \mathbf{r}}{2}\right)} \underset{H_0}{\overset{H_1}{\gtrless}} \gamma \quad (12)$$

As can be seen the only condition that is needed to decide in favor of one of the hypotheses is given by the following:

$$\mathbf{r}^T \mathbf{C}^{-1} \mathbf{g} \underset{H_0}{\overset{H_1}{\gtrless}} \gamma' \quad (13)$$

where $\mathbf{C}^{-1}\mathbf{g}$ are the MF weights.

This result is known as the Matched Filter for signal detection corrupted by zero-mean Gaussian noise. For white Gaussian noise, the covariance matrix $\mathbf{C}$ is diagonal and can be suppressed. As a result, the MF weights is the reference signal $\mathbf{g}$ itself. For the case where the Gaussian noise is correlated, the inverse of the covariance matrix has a pre-whitening function and the elements of the vector $\mathbf{C}^{-1}\mathbf{g}$ become the MF weights.

In TileCal, the shaper circuit output in the readout electronics provides a fixed and stable analog pulse and the energy is recovered from its amplitude. By taking the advantage of such pulse feature, the TileCal detection problem can be approximated as deterministic, which simplifies the MF implementation.

The acquired TileCal signal could be described by the components shown in Equation (14), where s_k is the received signal, ped is the baseline offset, n_k is the electronic noise, A is the amplitude and g_k is the TileCal reference pulse at a given time k.

$$s_k = ped + n_k + A g_k \quad (14)$$

Before the MF operation, the ped value is subtracted from the received sample s_k (periodically runs are taken in order to measure this quantity). Moreover, for filter design, the phase τ is considered zero (or fluctuates slightly) and the pulse peak is always centered at the fourth sample. As a result, the MF operation y between the incoming signal $\mathbf{s}$ and the MF coefficients is shown in Equation (15).

$$y = (\mathbf{s} - ped)^T \mathbf{C}^{-1} \mathbf{g} \quad (15)$$

It is worth mentioning that y is a single value and no longer corresponds to $\Lambda(\mathbf{r})$ from Equation (9). This is due to the fact that $\Lambda(\mathbf{r})$ is absorbed by γ' during the MF simplification, as expressed in Equation (13).

B. Amplitude estimation

The output from the detection operation shown in Equation (15) can be used to select signals with relevant information through the application of a simple threshold. However, it does not directly recover the input pulse amplitude, which is of interest as it guides to the final signal reconstruction. But Equation (15) can be restated as Equation (16) and the received signal amplitude can be computed by solving it for the variable A.

$$y = (\mathbf{n} + A\mathbf{g})^T \mathbf{C}^{-1} \mathbf{g} \tag{16}$$

This procedure leads to the expression shown by Equation (17), which is the estimation of the input pulse amplitude.

$$\hat{A}_{MF} = \frac{(\mathbf{s} - ped)^T \mathbf{C}^{-1} \mathbf{g}}{\mathbf{g}^T \mathbf{C}^{-1} \mathbf{g}} \tag{17}$$

Equation (17) shows an interesting property of the Matched Filter detector: the MF output can also be used as an amplitude estimator for TileCal. The numerator $(\mathbf{s} - ped)^T \mathbf{C}^{-1} \mathbf{g}$ is the usual MF operation, and the denominator $\mathbf{g}^T \mathbf{C}^{-1} \mathbf{g}$ is a constant that normalizes the MF operation in order to recover the signal amplitude in ADC counts unit.

IV. Results

Both MF and OF2 are currently designed (and implemented) for white Gaussian noise, therefore they perform close to their optimum operation when no Out-Of-Time (OOT) signal, or pile-up, is present and the background comprises only the electronic noise. This scenario is also called low luminosity condition as only one or a few interactions per Bunch-Crossing (BC) are expected. Figure 5 illustrates the current filter weights for a given TileCal channel.

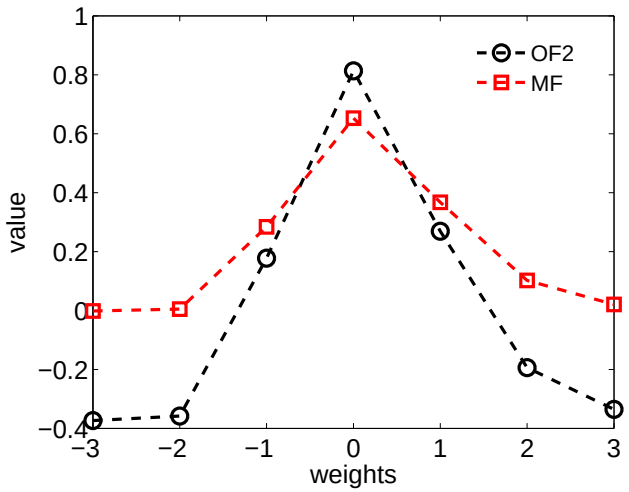

Fig. 5. OF2 weights (from minimization of Equation (7)) compared to MF weights (Equation (17)).

In the complementary scenario of high luminosity condition, the number of interactions per BC is higher and pile-up is observed. Under this scenario, the background contains the contribution of the usual electronic noise (Gaussian) as well as the pile-up (non-Gaussian). As a result, the background is no longer Gaussian and the methods decrease in performance by showing larger variance and higher bias.

In order to evaluate the performance of the MF and OF2 estimators, both low and high luminosities data acquired during LHC operation are used.

A. Performance on low luminosity data

Figure 6 shows the channel energy distribution reconstructed by the MF and OF2 algorithms using 2010 pp collision data at $\sqrt{s} = 7$ TeV, 150 ns bunch spacing (dT) and peak average number of interactions per crossing ($< \mu >$) of 3.31. Under these conditions the reconstruction is not affected by pile-up and the methods operate close to their optimum efficiency. However, OF2 shows a wider spread when compared to the MF around the noise region (±200 MeV). This spread can be seen as the estimation error (variance) of the methods. As energy increases we see a better agreement between methods, however, the absolute error remains the same, as it can be seen in Figure 7 where the correlation between the methods is shown.

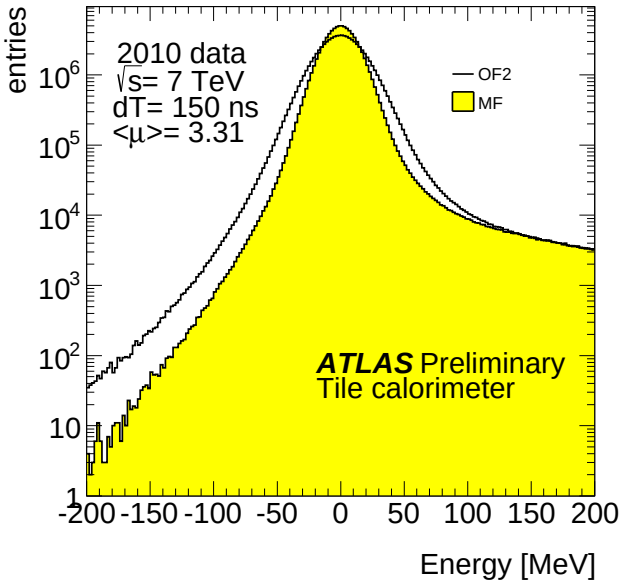

Fig. 6. Channel energy spectra for both OF2 and MF for low luminosity data.

B. Performance on high luminosity data

Similarly to the low luminosity data analysis, Figure 8 shows the channel energy distribution reconstructed by the MF and the OF2 algorithms using 2012 pp collision data at $\sqrt{s} = 8$ TeV, 25 ns bunch spacing (dT) and peak average number of interactions per crossing ($< \mu >$) of 11.3. Under such conditions, it can be seen the increase of the spread of the distribution obtained with both MF and OF2 with respect to the 2010 with 150 ns bunch spacing results. This increase

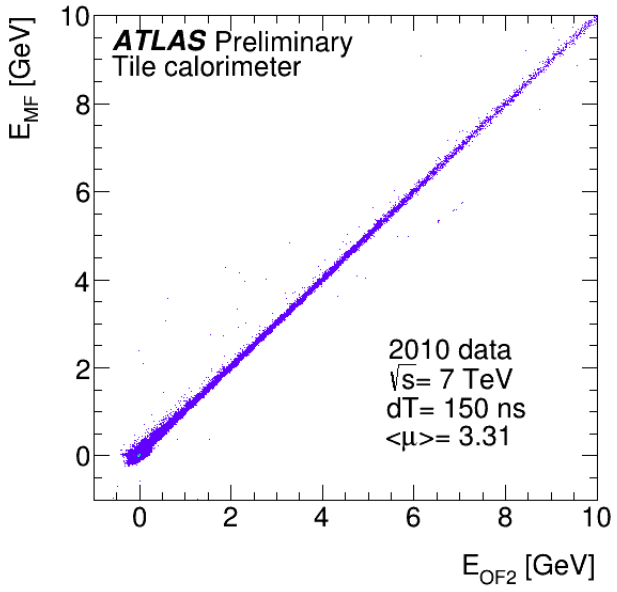

Fig. 7. Channel energy correlation between OF2 and MF for low luminosity data.

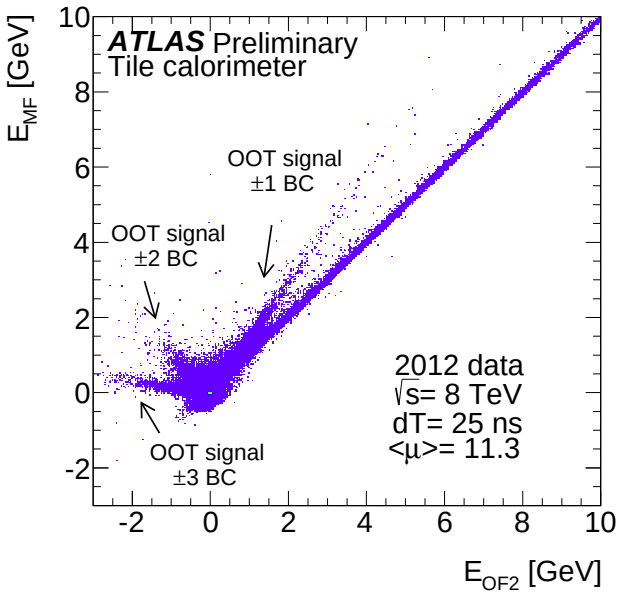

Fig. 9. Channel energy correlation between OF2 and MF for high luminosity data.

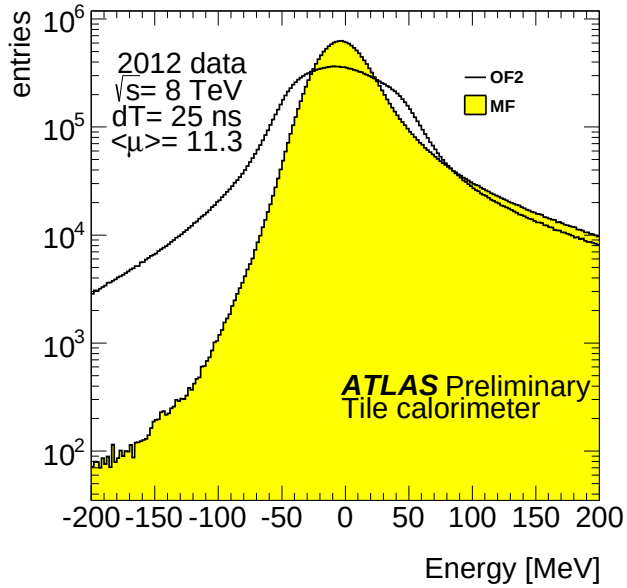

Fig. 8. Channel energy spectra for both OF2 and MF for high luminosity data.

is due to the presence of pile-up since the methods are not optimized for such conditions.

Concerning the linearity of the MF method, Figure 9 shows the correlation of channel energy. The contribution of OOT signals in the different BC are disentangled in this comparison. The OF2 systematically reconstructs smaller energies than the MF in the presence of OOT signals.

Due to the strong constraint of baseline immunity imposed by OF2 that forces the sum of the weights to be equal to zero (see Equation (6)), some of the OF2 weights have negative values (see Figure 5). As a result, in the presence of OOT signals at ± 3 BC or ± 2 BC, OF2 introduces negative bias to the final energy estimate while for an OOT signal at ± 1 BC, it introduces positive bias.

The MF estimator does not have the baseline immunity constraint, and its weights are all positive values. Therefore, in the presence of OOT signals it will always introduce positive bias. However, since the weights associated to the ± 3 BC and ± 2 BC are smaller than the OF2 ones, the bias introduced by the OOT signals are smaller for MF than for OF2. On the other hand, MF introduces larger positive bias with respect to OF2 for OOT signals located at ± 1 BC.

Both OF2 and MF can still make use of the noise covariance matrix in order to reduce the bias introduced by the pile-up. Yet, they will not be optimal as the background for high luminosity is not Gaussian.

It is worth mentioning that the MF method uses the likelihood ratio test to compute its weights. Therefore, it can be redesigned if the correct description of the pile-up is provided. However, the use of a non-Gaussian function is likely to lead to a non-linear estimator, which can be difficult to implement.

V. Conclusions

In this work, the TileCal Matched Filter algorithm for energy reconstruction was presented. The current performance of both the MF and OF2 was evaluated using collision data acquired during LHC operation. For low luminosity conditions, the MF showed smaller estimation error and is highly correlated with OF2 for high SNR signals. In other hand, both methods decrease in performance as the LHC luminosity increases. This can be explained by the bias introduced in the estimators since they are not optimized for such conditions. Moreover, the presence of OOT signals leads to a non-Gaussian background, therefore, an increase in variance is also expected.

In order to deal with the pile-up, the usage of the covariance matrix to compute the filter weights are under evaluation, since the current implementation assumes that the background is uncorrelated between samples and Gaussian distributed. This approach can reduce the effect of the pile-up, however, it still will not use the correct description of the noise. Moreover, both the signal baseline and the covariance matrix changes according to the level of pile-up, which can make the online implementation difficult.

A deconvolution based approach has also been considered. It assumes the incoming signal as a linear mixture of OOT signals and it finds a transformation that recovers each one of the OOT signal amplitudes. The main advantage of this technique is the fact that the background comprises only the electronic noise regardless the luminosity.

ACKNOWLEDGMENT

I would like to thank the TileCal group for the fruitful discussion concerning this work.

REFERENCES

[1] The ATLAS Collaboration, *The ATLAS Experiment at the CERN Large Hadron Collider*, Journal of Instrumentation, JINST 3 S08003, 2008.

[2] The ATLAS Collaboration, *Readiness of the ATLAS Tile Calorimeter for LHC collisions*, EPJC 70, 1193-1236, 2010.

[3] Kordas, K., Abolins, M. et al. *The ATLAS Data Acquisition and Trigger: concept, design and status*, Nuclear Physics B - Proceedings Supplements, vol. 172, pp. 178-182, 2007.

[4] K. Anderson *et al.*, *Front-end Electronics for the ATLAS Tile Calorimeter*,Proceedings of Fourth Workshop on Electronics for LHC Experiments, Rome, 1998.

[5] M. Tylmad *et al*, *Pulse shapes for signal reconstruction in the ATLAS Tile Calorimeter*, Proc. Real Time Conference RT'09 (Beijing). 16th IEEE-NPSS, pp 543-547, 2009.

[6] G. Bertuccio, E. Gatti and M. Sapietro, *Sampling and optimum data processing of detector signals*, Nuclear Instruments and Methods in Physics Research A, v. 322, 271 - 279, 1992.

[7] WE. Cleland, E.G. Stern, *Signal processing considerations for liquid ionization calorimeters in a high rate environment*, Nucl. Instr. and Meth. in Phys. Res. A 338, 467-497, 1994.

[8] M. Delmastro, *A stand-alone signal reconstruction and calibration algorithm for the ATLAS electromagnetic calorimeter*, 2003 IEEE Nuclear Science Symposium Conference Record, pp.1110-1114, Vol.2, 2003.

[9] E. Fullana *et. al.*, *Digital Signal Reconstruction in the ATLAS Hadronic Tile Calorimeter*, IEEE Transaction On Nuclear Science, v. 53, number 4, 2006.

[10] H. L. V. Trees, *Detection, Estimation and Modulation Theory, Part I*, Wiley, 2001.

[11] G. L. Turin, *An introduction to digitial matched filters*, Proceedings of the IEEE , vol.64, no.7, pp.1092-1112, 1976.